



## REDUCTION OF OPTICAL NOISE IN NEAR-INFRARED RANGE LASER HYGROMETRY

Tadeusz Stacewicz, Mateusz Winkowski, Natalia Kuk

*Institute of Experimental Physics, Faculty of Physics, University of Warsaw, 02-093 Warsaw, Pasteura 5, Poland*  
(✉ [mateusz.winkowski@fuw.edu.pl](mailto:mateusz.winkowski@fuw.edu.pl), [tadeusz.stacewicz@fuw.edu.pl](mailto:tadeusz.stacewicz@fuw.edu.pl))

### Abstract

A contactless laser hygrometer based on light absorption by H<sub>2</sub>O molecules at 1392.5 nm is described. However, measurement results can be affected by optical noise when applied to an atmospheric tunnel or glass cuvette. The noises (occurring in the form of periodic fringes in the recorded spectrum) come from unexpected interference of the light beams reflected from surfaces of the windows or other optical elements. The method of their suppression is described in this article. It is based on wavelength modulation and signal averaging over the fringes period. Also, an experiment confirming the usefulness of this method is described here.

Keywords: hygrometer, laser, absorption spectroscopy, optical interference.

© 2023 Polish Academy of Sciences. All rights reserved

### 1. Introduction

Measurements of H<sub>2</sub>O concentration in gases are widely used in various applications, from technological ones and geophysical research to the determination of water vapour in human breath. Different humidity meters have been developed for this purpose. Besides various popular instruments, highly accurate dew point devices, psychrometers, thin-film capacitance meters, and many others are also included in the group characterized by fast response [1]. Nevertheless, all these sensors require water deposition from the investigated gas. Such a solution makes the humidity measurement work with relatively pure temporal resolution.

The determination of the water vapor density by measuring light quenching in the investigated sample provides an opportunity to avoid such a disadvantage and achieve a time resolution better than 1 ms. The most sensitive solutions of this type use laser radiation tuned to strong absorption lines of water molecules [1–4]. Additionally, the application of ultrasensitive techniques of laser absorption spectroscopy, such as *cavity ring-down spectroscopy* (CRDS) or multipass spectroscopy, provides the opportunity to achieve a molecular detection limit as low as 10<sup>10</sup> cm<sup>-3</sup> [5].

Copyright © 2023. The Author(s). This is an open-access article distributed under the terms of the Creative Commons Attribution-NonCommercial-NoDerivatives License (CC BY-NC-ND 4.0 <https://creativecommons.org/licenses/by-nc-nd/4.0/>), which permits use, distribution, and reproduction in any medium, provided that the article is properly cited, the use is non-commercial, and no modifications or adaptations are made.

Article history: received August 13, 2022; revised October 18, 2022; accepted November 16, 2022; available online February 2, 2023.

In our previous papers, we presented a *fast infrared hygrometer* (FIHR) based on observation of radiation absorption [6]. Its huge advantage consists in remote measurement of H<sub>2</sub>O concentration, without any contact with the investigated gas, using a weak laser beam, thus providing an opportunity to avoid disturbance of the sample. This single-pass device is suitable for determination of absolute concentration of water molecules in air with a sensitivity of 10<sup>14</sup> cm<sup>-3</sup>. Temporal resolution better than 10<sup>-2</sup> s might be achieved. [5]. A comparison of its parameters with properties of commercially available instruments was presented in Table 1.

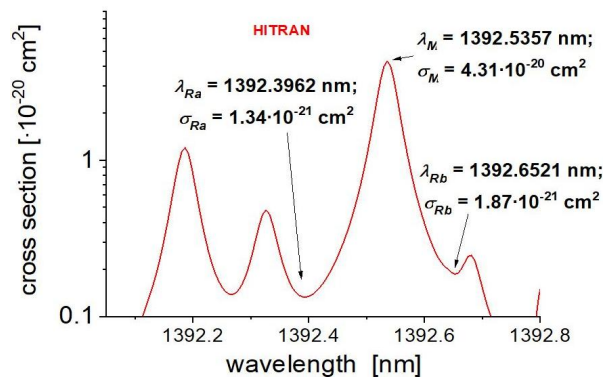
Previously, the hygrometer was used for free-air surrounding. Recently, the sensor was applied for humidity analysis in an atmospheric tunnel [7,8]. We stated that in this case the recorded H<sub>2</sub>O absorption spectrum is affected by optical interference which occurs when the laser light is transmitted through the tunnel windows. In this paper, we present an approach providing an opportunity to reduce such disadvantage. The usefulness of this method was confirmed experimentally.

Table 1. Comparison of parameters of selected hygrometers.

Hygrometer	Manufacturer	Sensitivity	Reaction Time	Measurement
LI-7500A	LI-COR Inc.	5 · 10 <sup>14</sup> cm <sup>-3</sup>	5 · 10 <sup>-2</sup> s	CO <sub>2</sub> /H <sub>2</sub> O; open path gas analysis
KH20	Campbell Scientific	5.7 · 10 <sup>16</sup> cm <sup>-3</sup>	10 <sup>-2</sup> s	krypton hygrometer; absolute H <sub>2</sub> O concentration
Model 973 Dew Point Mirror	RH Systems LCC	5% < RH < 100%	1 s	relative humidity
laser hygrometer	this work	10 <sup>14</sup> cm <sup>-3</sup>	< 10 <sup>-2</sup> s	absolute H <sub>2</sub> O concentration; contactless

## 2. Principles of optical hygrometry

The operation of FIHR was described in detail in our previous papers [5,6]. Briefly, it is based on the measurement of laser light quenching by water molecules present in the investigated sample. The laser is tuned to the specific rovibronic H<sub>2</sub>O line in the near infrared range. At this wavelength ( $\lambda_M$ ) the transmission through the investigated sample is compared with that at a reference wavelength  $\lambda_R$  (Fig. 1).

Fig. 1. Absorption spectra of the H<sub>2</sub>O molecule applied for FIHR.

The line with the peak wavelength at  $\lambda_M = 1392.5357$  nm characterized by the cross section of  $\sigma_M = 4.31 \cdot 10^{-20}$  cm<sup>2</sup> was selected for our hygrometer [9]. There are two minima in the neighbourhood of this line: one at the wavelength  $\lambda_{Ra} = 1392.3962$  nm with the cross section  $\sigma_{Ra} = 1.34 \cdot 10^{-21}$  cm<sup>2</sup> and the other one at  $\lambda_{Rb} = 1392.6521$  nm ( $\sigma_{Rb} = 1.33 \cdot 10^{-21}$  cm<sup>2</sup>).

### 3. Sensor construction

The scheme of the FIRH sensor is presented in Fig. 2. A single mode semiconductor laser (Toptica, DL100) serves as a source of monochromatic light. The tuning of the laser is performed with current and temperature controllers which keep the wavelength at  $\lambda_M$  or  $\lambda_R$  values respectively. The laser beam is conducted in a fiber and then splits twice in the couplers (Thorlabs, FC 13007099). Coupler C<sub>1</sub> directs a portion of the beam (about 1% in intensity) into the wavemeter (HighPrecision, WS6) which is used for tuning the wavelength to the desired value with a precision of 0.001 nm.

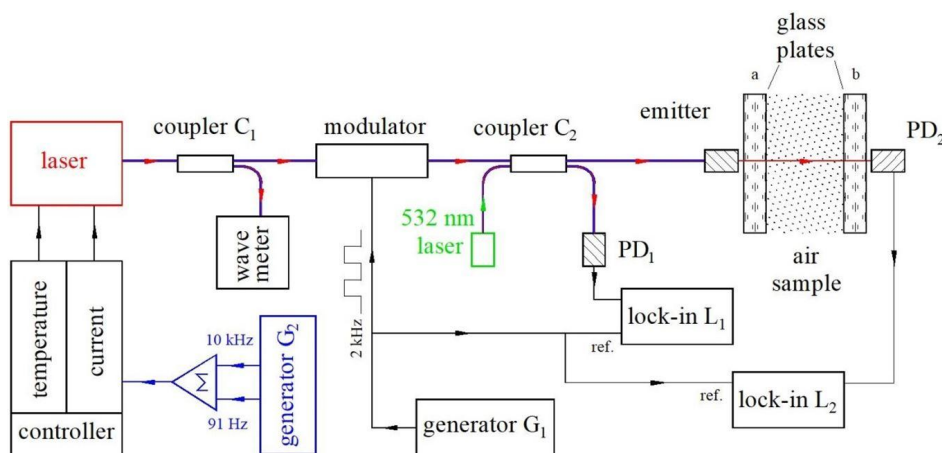


Fig. 2. Scheme of the FIRH. Fibers are sketched in violet, light beams are in red, appropriate cabling is in black. The equipment sketched in blue was added to the system for reduction of optical interference.

The main beam leaving coupler C<sub>1</sub> is sent to the electro-optical modulator (Jena), providing modulation of light intensity. The modulator is driven by generator G<sub>1</sub> (Tektronix, AGF 3102) working at a frequency of 2 kHz. Coupler C<sub>2</sub> sends a portion of the beam (about 1%) to photodiode PD<sub>1</sub> (G8370 03) that monitors the laser power<sup>1</sup>. The dominant beam is guided from C<sub>2</sub> to an emitter that sends light to the air sample. The intensity of the beam transmitted through the sample is measured with another photodiode (PD<sub>2</sub>). Signals generated by photodiodes PD<sub>1</sub> and PD<sub>2</sub> are recorded with a two lock-in amplifier (Stanford Research Systems, SR830).

The two-step measurement procedure is applied. In the first step, the laser is tuned to the  $\lambda_M$  wavelength and the respective signals  $I_{M1}$  and  $I_{M2}$  from the photodiodes PD<sub>1</sub> and PD<sub>2</sub> are recorded. Then the wavelength is tuned to one of  $\lambda_R$  values and the reference signals  $I_{R1}$  and  $I_{R2}$  from the respective photodetectors are stored. The mean concentration of H<sub>2</sub>O molecules ( $n_H$ ) that are present along distance  $L$  between the emitter and the PD<sub>2</sub> photodiode is determined using

<sup>1</sup>Coupler C<sub>2</sub> is also used to merge 532 nm laser radiation to the fibre. This beam is applied only for system adjustment.

a formula following the Lambert–Beer law:

$$n_H = \frac{1}{L(\sigma_M - \sigma_R)} \ln \left( \frac{I_{R2} I_{M1}}{I_{R1} I_{M2}} \right). \quad (1)$$

It is worth pointing out that this measurement is sensitive only for the concentration of molecular water, while the influence of light scattering on dust or water droplets is ignored due to simultaneous registration at both  $\lambda_M$  and  $\lambda_R$ .

#### 4. Optical interferences

The simple approach (1) to determination of water vapour density can be applied only to the measurement in the free atmosphere. In the case of registration through windows (in tunnels, cuvettes, *etc.*) one can expect optical interference, which convolves the absorption spectrum. This disturbance is not caused by light absorption or scattering in glass since these processes do not modify the ratios between  $I_{M2}$  and  $I_{R2}$  signals due to flatness of such spectra within the wavelength range used in this hygrometer. However, the multiply beam reflections inside the glass plates and their overlapping lead to light interferences and occurring of periodic oscillations in the transmission spectrum (Fig. 3). These optical fringes may affect the argument of logarithm function in (1) because the intensity variation of  $I_{M2}$  and  $I_{R2}$  may be not equal. For a single plate, the fringes are described by formula [10]:

$$T_1(\lambda) = \left[ 1 + \frac{4R}{(1-R)^2} \sin^2 \left( \frac{2\pi dn}{\lambda} + \Delta\varphi \right) \right]^{-1}, \quad (2)$$

where  $d$  and  $n$  denote the glass thickness and the refraction coefficient, respectively. The reflection coefficient of the glass surface is equal to  $R = (1-n)^2/(1+n)^2$  assuming perpendicular incidence of the light beam on the plate surface. Phase shift  $\Delta\varphi$  follows from uncertainty of the plate thickness.

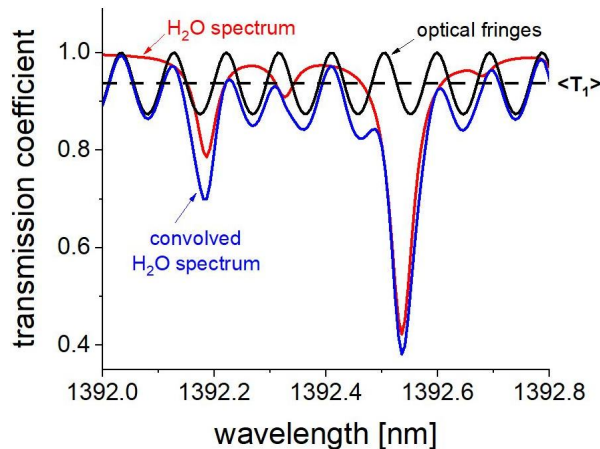


Fig. 3. Example of an optical fringes spectrum that occurs in transmission through a single glass plate and its convolution with the H<sub>2</sub>O absorption spectrum [9].

One can easily calculate that for typical floated borosilicate glass with a refraction coefficient of  $n = 1.47$ , the reflection coefficient is equal to  $R = 3.6\%$  [11]. Then the transmission of a

single glass oscillates within quite a large range of  $0.865 < T_1 \leq 1$  around the mean value  $\langle T \rangle = (1 - R)^2 = 0.929$  (Fig. 3). The fringes lead to a strong modification of the transmitted spectrum. This belongs to the most important effects disturbing such optical measurements.

An example of the fringes that can occur in the spectral range near 1392.5 nm in light transmitted through a single glass plate of  $d = 7$  mm (which was used in the experiment described below) is presented in Fig. 3. The oscillation period

$$\Delta\lambda \approx \frac{\lambda^2}{(2nd)} \quad (3)$$

reaches a value of about 0.09 nm. However, the fringe phase shift  $\Delta\varphi$  is usually unknown. It can vary just as the consequence of uncertainty of separation of the reflecting surfaces. The variation over one period ( $2\pi$ ) takes place for uncertainty  $\Delta d_{2\pi} = \lambda/2n$ . The typical uncertainty of the thickness of the plate reaches  $\Delta d = \pm 0.3$  mm for a glass of 7 mm in thickness [12], *i.e.*, it is about 75 times larger than  $\Delta d_{2\pi}$ . Therefore,  $\Delta\varphi$  can strongly change from point to point of the window. The phase shift is also thermally unstable. The thermal expansion coefficient for borosilicate glass is about  $3.3 \cdot 10^{-6} \text{ K}^{-1}$ , then the phase variation over radians can occur at the temperature changes in the range of tens of kelvins. The huge uncertainty of  $\Delta\varphi$  causes that in practice this kind of noise cannot be effectively compensated during data post-processing, using the fringe spectrum recorded when testing the experimental system.

Various well-known methods are used for such interference reduction. Anti-reflection coatings on the glass surfaces or the application of wedge or thick optical windows that are tilted in respect to the incident light beam belong to them. All these solutions are useful for small cuvettes, but they are not applicable for apparatuses like the atmospheric tunnels with large windows, where the hygrometer position is scanned over distances of tens of centimetres in respect to the air flux [8, 9]. In this case, the laser beam passes through two similar glass plates (we denote them by the indexes  $a$  and  $b$  – see Fig. 2). Then the effective transmission coefficient is equal<sup>2</sup>:

$$T_2(\lambda) = T_a(\lambda)T_b(\lambda) = \left[ 1 + \frac{4R}{(1-R)^2} \sin^2 \left( \frac{2\pi dn}{\lambda} + \Delta\varphi_a \right) \right]^{-1} \left[ 1 + \frac{4R}{(1-R)^2} \sin^2 \left( \frac{2\pi dn}{\lambda} + \Delta\varphi_b \right) \right]^{-1}. \quad (4)$$

Examples of these functions are shown in Fig. 4. For two borosilicate glasses considered above [11], the transmission can vary around the mean value of  $\langle T_2 \rangle = (1 - R)^4 = 0.863$  within the range of  $0.748 < T_2 \leq 1$ , however, oscillation amplitude and phase depend on the difference of the phase shifts in both plates:  $\Delta\varphi_b - \Delta\varphi_a$ . The oscillation period is similar to the single glass:  $\Delta\lambda = \lambda^2/(2nd)$ . The frequencies of Fourier harmonics of the  $T_2$  function (4) are the same as for  $T_1$  (2).

It is evident that in both cases presented above optical interference can lead to huge distortions in the transmitted light spectrum. No precise determination of the light intensities at  $\lambda_M$  and  $\lambda_R$  wavelengths (1) is possible. This severely spoils optical measurements of water vapour concentration.

<sup>2</sup>We assume that the glass plates are separated by tens of centimeters. Thus, for the narrow laser beam (with a diameter of 3 mm) and its tilting in respect to normal to the glass surfaces by several degrees, the beams reflected from different plates do not overlap.

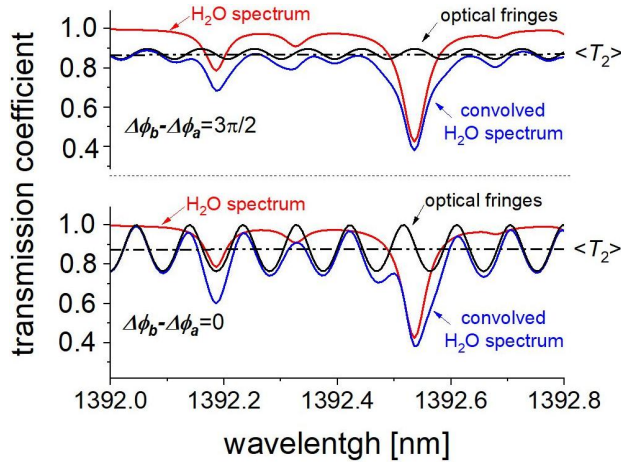


Fig. 4. Examples of the spectrum of optical noise in transmission through two glasses and their convolution with the H<sub>2</sub>O absorption spectrum for two cases of relative phase shifts [9].

### 5. Wavelength modulation as a method for fringe interference suppression

Besides the passive methods of the fringe suppression, which were presented above, various active approaches have been undertaken by several groups. In multipass spectroscopy it consisted in periodic shifting of the mirrors by pressure or piezoelectric elements [12–14]. Oscillating Brewster plates or lenses are also used [15, 16] as well as wavelet transforms [17]. This method spoils the stability of the interference fringes, so it reduces them when averaging the light transmitted through the cell; however, it leads to system complication. Using of laser wavelength modulation over a certain spectral range and adjacent averaging of the signal transmitted through the window(s) proves more convenient. This idea was already shown for multipass cells [18–20]. We have pointed out that this approach is especially efficient when additional modulation and averaging are performed over the fringes period [21].

The adjacent (running) averaging operation on function  $f(\lambda)$  can be expressed by the equation:

$$\langle f(\lambda, D_\lambda) \rangle = \frac{1}{D_\lambda} \int_{\lambda - \frac{D_\lambda}{2}}^{\lambda + \frac{D_\lambda}{2}} f(x) dx, \quad (5)$$

where  $(D_\lambda)$  denotes the range of averaging. This is widely used as a method of data smoothing during the post-processing of the experimental results. In electronics it is known as a digital windowed sinc filter [22, 23]. Its transmission spectrum was shown in Fig. 5. The filter very effectively quenches the periodic functions at resonance frequencies, i.e., which periods  $\Delta_\lambda$  are matched with the averaging range  $D_\lambda$  according to relation:  $D_\lambda/\Delta_\lambda = 1, 2, 3 \dots$

Since the transmission of two glass plate system is a periodic function (4), then it can be expressed in the form:

$$T_2(\lambda) = (1 - R)^4 + \sum_{k=1}^{\infty} A_k \sin \left( k \frac{2\pi\lambda}{\Delta_\lambda} + \psi_k \right), \quad (6)$$

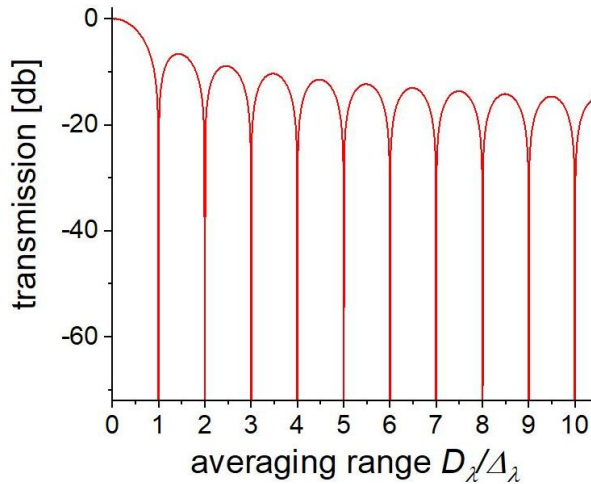


Fig. 5. Transmission spectrum of the adjacent averaging filter.

where  $A_k$  and  $\psi_k$  denote the amplitude and the phase shift of the harmonic  $k$ , respectively. Their period is  $\Delta_{\lambda k} = \Delta_{\lambda}/k$ . Adjacent averaging leads to elimination of the second formula consisting of the harmonic functions when the resonance condition (mentioned in the previous paragraph) is fulfilled.

The results of interference quenching are presented in Fig. 6. Changes in transmission as a function of the averaging range are shown for various differences in the phase shifts in both plates ( $\Delta\phi_b - \Delta\phi_a$ ). The most effective is averaging over the wavelength range equal to the multiplicity of the fringe period ( $D_{\lambda}/\Delta_{\lambda} = 1, 2, 3 \dots$ ) since in this case the transmission does not depend on the phase shift; it is equal to the mean value  $\langle T_2 \rangle = (1 - R)^4$ .

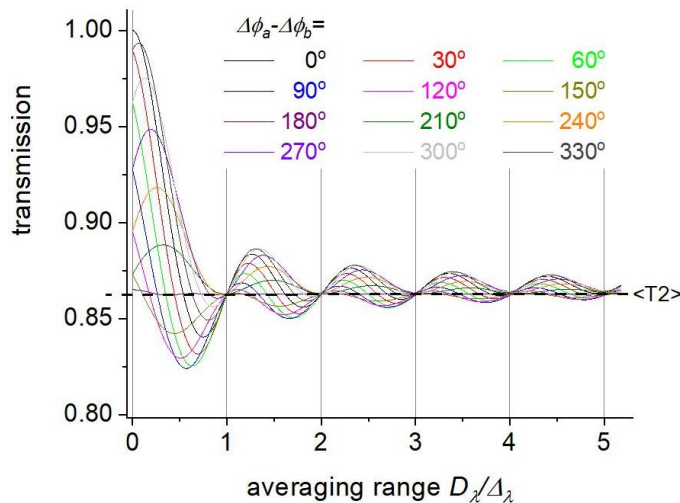


Fig. 6. Quenching of fringes occurring during the transmission through two plates due to wavelength modulation and signal averaging for various phase-shift differences.

In our hygrometer (Fig. 2), the light intensity that is transmitted through the glass plates and the vapor layer is equal:

$$\begin{aligned}
 I(\lambda) &= I_0(\lambda)T_2(\lambda) \exp[-\sigma(\lambda)n_H L] \\
 &= I_0(\lambda) \left[ (1-R)^4 + \sum_{k=1}^{\infty} A_k \sin\left(k \frac{2\pi\lambda}{D_\lambda} + \psi_k\right) \right] \exp[-\sigma(\lambda)n_H L], \quad (7)
 \end{aligned}$$

where  $I_0(\lambda)$  denotes the intensity of the beam leaving the emitter. For a weak absorption coefficient ( $\sigma(\lambda)n_H L \ll 1$ ), the exponent can be replaced by a polynomial of first order. The application of adjacent averaging to  $I(\lambda)$  and the assumption that the laser intensity changes only slightly when its wavelength is tuned over the oscillation period ( $I_0(\lambda) \approx \text{const}$ ), leads to the following equation:

$$\langle I(\lambda) \rangle \approx \frac{I_0(\lambda)}{D_\lambda} \int_{\lambda - \frac{D_\lambda}{2}}^{\lambda + \frac{D_\lambda}{2}} \left[ (1-R)^4 + \sum_{k=1}^{\infty} A_k \sin\left(k \frac{2\pi x}{D_\lambda} + \psi_k\right) \right] [1 - \sigma(x)n_H L] dx. \quad (8)$$

According to the filter spectrum (Fig. 5) the integration over the period (or multiplicity of the period) leads to elimination of the expression:

$$\frac{I_0(\lambda)}{D_\lambda} \sum_{k=1}^{\infty} \int_{\lambda - \frac{D_\lambda}{2}}^{\lambda + \frac{D_\lambda}{2}} A_k \sin\left(k \frac{2\pi x}{D_\lambda} + \psi_k\right) dx \longrightarrow 0. \quad (9)$$

Moreover, the expression:

$$\frac{I_0(\lambda)}{D_\lambda} \sum_{k=1}^{\infty} \int_{\lambda - \frac{D_\lambda}{2}}^{\lambda + \frac{D_\lambda}{2}} A_k \sin\left(k \frac{2\pi x}{D_\lambda} + \psi_k\right) \sigma(x)n_H L dx \quad (10)$$

providing additional Fourier harmonics is also negligible due to weakness of the absorption coefficient and due to the fact that the sinc filter transmission quenches also at the frequencies below the resonant ones. Finally, one achieves:

$$\langle I(\lambda) \rangle \approx (1-R)^4 I_0(\lambda) \left[ 1 - \frac{n_H L}{D_\lambda} \int_{\lambda - \frac{D_\lambda}{2}}^{\lambda + \frac{D_\lambda}{2}} \sigma(x) dx \right] = I_0(1-R)^2 [1 - n_H L \langle \sigma(\lambda) \rangle], \quad (11)$$

where

$$\langle \sigma(\lambda) \rangle = \frac{1}{D_\lambda} \int_{\lambda - \frac{D_\lambda}{2}}^{\lambda + \frac{D_\lambda}{2}} \sigma(x) dx \quad (12)$$

denotes the effective cross section, i.e., the mean value of the cross section over the modulation period.

The modulation and averaging of the laser wavelength over a certain wavelength range lead to changes in the recorded absorption spectrum. Such a transformation (flattening and broadening of the lines) for water spectrum was shown in Fig. 7 for the 1392.5 nm absorption line. Here the averaging was done within the range of  $\Delta\lambda = 90.4$  pm which corresponds to the period of the fringe spectrum produced by 7 mm borosilicate glasses (already calculated in Section 4). Moreover, changes in the wavelengths and the cross sections corresponding to maxima and minima of the effective absorption spectrum occur with respect to the original spectrum.

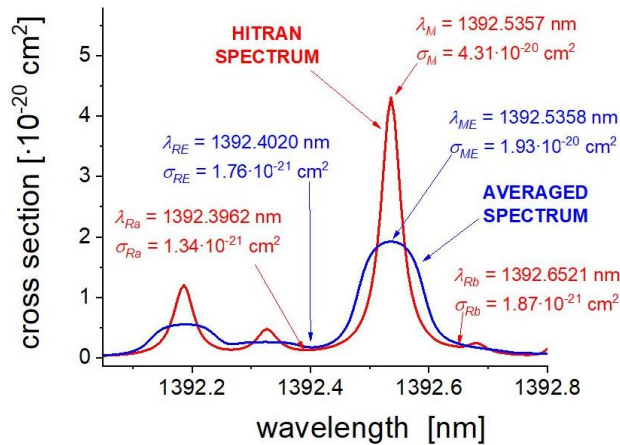


Fig. 7. Changes in the H<sub>2</sub>O absorption spectrum due to adjacent averaging over 90.4 pm.

For example, the wavelength corresponding to the minimal local cross section  $\lambda_{RE}$  was shifted by about 0.0139 nm toward shorter wavelengths with respect to  $\lambda_{Ra}$ . The corresponding value of the effective cross section  $\sigma_{RE}$  rose by a factor of 1.3 with respect to  $\sigma_{Ra}$ . The second minimum at the wavelength  $\lambda_{Rb}$  disappeared due to the averaging process. The maximum effective absorption spectrum  $\lambda_{ME}$  was practically not shifted (1392.5358 nm), but the value of the maximum effective cross section maximum ( $\sigma_{ME}$ ) decreased approximately 2.2 times with respect to  $\sigma_M$ . Such changes of the effective cross sections must be taken into account when calculating the absorber concentration with (1).

## 6. Experiment

In order to check the effectiveness of the method of fringe suppression an experiment was performed in which we used the system of water vapour detection presented in Fig. 2. The setup was slightly modified in respect to that presented in Fig. 2 since a two-channel function generator (JDS 6600 from JOY iT) was additionally used for laser tuning and modulation. The output signals from both channels were combined in a custom summing amplifier ( $\Sigma$  in Fig. 2). The amplifier output was used to drive the laser current. The first channel (generating at the frequency of 91 Hz) served as the laser wavelength switch between the maximum ( $\lambda_{ME}$ ) and minimum ( $\lambda_{RE}$ ) in the H<sub>2</sub>O spectrum. The second channel (with the 10 kHz signal) was used for quenching optical interference. Its amplitude (*i.e.*, the amplitude of laser wavelength modulation) was manually tuned to the value corresponding to the best quenching of the optical interference, *i.e.* the period of the optical fringes.

During the experiment two glass plates were located between the emitter and the photodiode PD<sub>2</sub>. The distance between the plates was about 80 cm<sup>3</sup>. The glasses were parallel each to the other. The laser beam was tilted by several degrees in respect to normal to the glass surfaces in order to avoid interference between the plates. The measurement was carried out in free air at a temperature of 23°C and a relative humidity of about 40%. Using an improved Magnus approximation allows us to calculate the saturated vapor pressure, one can evaluate that during the experiment the H<sub>2</sub>O density was about  $n_{\text{exp}} \approx 2.76 \cdot 10^{17} \text{ cm}^{-3}$  [24].

The results of the measurements are presented in Fig. 8. The red curve (the reference transmission spectrum of water vapor) was calculated using the HITRAN data base for the  $n_{\text{exp}}$  concentration [9]. The black curve shown below (the convolved spectrum) was recorded when two glass plates were placed between the fibre emitter and the photodiode PD<sub>2</sub> (Fig. 2). In this case the 10 kHz generator (causing the wavelength modulation) was switched off. The spectrum evidently differs from the reference one since it was convolved by the fringes arising in plates due to the interference. The fringe period ( $\Delta\lambda \approx 90 \text{ pm}$ ) corresponds well to the theoretically predicted period of the noises which are generated in glass plates of 7 mm in thickness. Such spectrum is useless for correct water vapor density determination since in this case the  $I_{M2}/I_{M1}$  and  $I_{R2}/I_{R1}$  ratios (which are necessary when using the (1)) cannot be found properly.

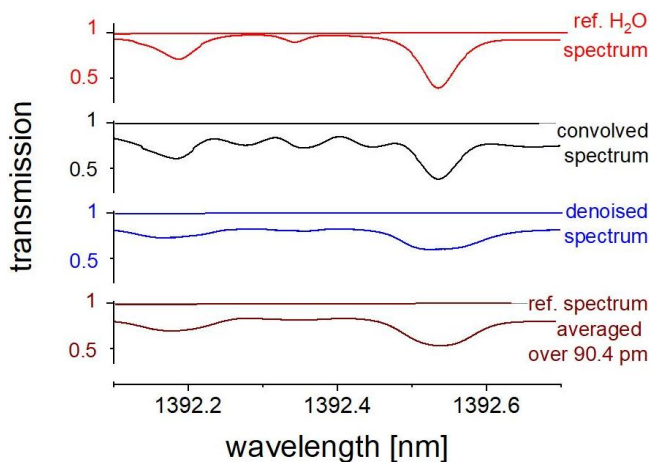


Fig. 8. Water absorption lines interfered after passing by two perpendicularly aligned glass plates (solid blue line) and averaged the spectrum after the use of the optical interference suppression.

In Fig. 8 the blue curve (“denoised spectrum”) represents the spectrum recorded when both, the wavelength modulation by the 10 kHz signal and the averaging were used. Efficient elimination of the fringes is observed. However, the flattening of the H<sub>2</sub>O spectrum (predicted in a previous chapter) also occurs. The shape of the denoised spectrum corresponds well to the reference spectrum (wiggly line shown below) from the Hitran data base recalculated using (11) and (12). In this case the smoothing of the cross section was done with adjacent averaging over the range of  $D_\lambda = 90.4 \text{ pm}$ .

Suppression of interference allows us to find the values of  $I_{M2}/I_{M1}$  at  $\lambda_M$  and  $I_{R2}/I_{R1}$  at  $\lambda_{RE}$  using the denoised spectrum. This provides the opportunity to calculate the H<sub>2</sub>O concentration

<sup>3</sup>Separation of the plates by 80 cm was chosen to simulate experimental circumstances similar to those of the LACIS-T atmospheric tunnel [6, 7].

using (1), however, the effective cross sections  $\langle\sigma_{ME}\rangle$  and  $\langle\sigma_{RE}\rangle$  have to be used (12). The achieved result  $n_H \approx 2.79 \cdot 10^{17} \text{ cm}^{-3}$ , that was calculated in this way, is in good agreement with the  $n_{\text{exp}}$  value determined with the Magnus formula [22].

## 7. Conclusions

We presented an approach for contactless optical measurement of water concentration in air. It is based on the investigation of laser light quenching and the Lambert–Beer law. The results of such experiment can be affected by huge errors when the investigated area is separated from the optical equipment by glass windows (in cells or the atmospheric tunnels, *etc.*). In this case, the recorded spectrum of H<sub>2</sub>O vapour convolves with the interference fringes, which arise in the glass plates. The method of suppression of such optical noise was described. It consists in laser wavelength modulation and data averaging over the fringes period. Such approach provides opportunity to solve the fringes problem in the cases described in Section 3.2, *i.e.*, when their phase shift is unknown or thermally unstable.

For the first time theoretical analysis of such approach was presented in this paper. It was shown that the method interacts on the experimental data in a way similar as the case of the application of the *sinc filter* for alternating signals [20, 21]. Using of such a filter leads to the most efficient suppression of the periodic interference when the amplitude of the wavelength modulation is equal to the fringes period. It was noticed, however, that such processing of the signal also leads to flattening of the recorded spectra. We have shown that despite this distortion the proper determination of the absorber concentration is possible using the Lambert–Beer approximation (1). It requires using of the cross sections that are smoothed in the same way, *i.e.*, averaged over the period of the noise fringes. The results of the theoretical analysis were confirmed in the experiment.

The approach presented in this paper can be applied to eliminate analogous optical interference in various optical systems.

## References

- [1] Korotcenkov, G. (2018). *Handbook of Humidity Measurement, Volume 1: Spectroscopic Methods of Humidity Measurement*. CRC Press.
- [2] Abe, H., & Yamada, K. M. (2011). Performance evaluation of a trace-moisture analyzer based on cavity ring-down spectroscopy: Direct comparison with the NMIJ trace-moisture standard. *Sensors and Actuators A: Physical*, 165(2), 230–238. <https://doi.org/10.1016/j.sna.2010.11.005>
- [3] Buchholz, B., Böse, N., & Ebert, V. (2014). Absolute validation of a diode laser hygrometer via intercomparison with the German national primary water vapor standard. *Applied Physics B*, 116(4), 883–899. <https://doi.org/10.1007/s00340-014-5775-4>
- [4] Filges, A., Gerbig, C., Rella, C. W., Hoffnagle, J., Smit, H., Krämer, M., & Ebert, V. (2018). Evaluation of the IAGOS-Core GHG package H<sub>2</sub>O measurements during the DENCHAR airborne inter-comparison campaign in 2011. *Atmospheric Measurement Techniques*, 11(9), 5279–5297. <https://doi.org/10.5194/amt-11-5279-2018>
- [5] Stacewicz, T., & Magryta, P. (2018). Highly sensitive airborne open path optical hygrometer for upper air measurements – proof of concept. *Metrology and Measurement Systems*, 793–805. <https://doi.org/10.24425/mms.2018.124877>

- [6] Nowak, J. L., Magryta, P., Stacewicz, T., Kumala, W., & Malinowski, S. P. (2016). Fast optoelectronic sensor of water concentration. *Optica Applicata*, 46(4), 607–618. <https://doi.org/10.5277/oa160408>
- [7] Grosz, R., Nowak, J., Niedermeier, D., Mijas, J., Frey, W., Ort, L., & Voigtländer, J. (2021, March). Contactless and high-frequency optical hygrometry in LACIS-T. In *EGU General Assembly Conference Abstracts* (pp. EGU21-14538).
- [8] Nowak, J. L., Grosz, R., Frey, W., Niedermeier, D., Mijas, J., Malinowski, S. P., Ort, L., Schmalfuß, S., Stratmann, F., Voigtländer, J., & Stacewicz, T. (2022). Contactless Optical Hygrometry in LACIS-T. *Atmospheric Measurement Techniques*, 15, 4075–4089. <https://doi.org/10.5194/amt-15-4075-2022>
- [9] Rothman, L. S., Gordon, I. E., Babikov, Y., Barbe, A., Benner, D. C., Bernath, P. F., & Wagner, G. (2013). The HITRAN2012 molecular spectroscopic database. *Journal of Quantitative Spectroscopy and Radiative Transfer*, 130, 4–50. <https://doi.org/10.1016/j.jqsrt.2013.07.002>
- [10] Demtröder, W. (2013). *Laser spectroscopy: Basic Concepts and Instrumentation*. Springer Science & Business Media.
- [11] Luo, J., Smith, N. J., Pantano, C. G., & Kim, S. H. (2018). Complex refractive index of silica, silicate, borosilicate, and boroaluminosilicate glasses – Analysis of glass network vibration modes with specular-reflection IR spectroscopy. *Journal of Non-Crystalline Solids*, 494, 94–103. <https://doi.org/10.1016/j.jnoncrysol.2018.04.050>
- [12] Fried, A., Drummond, J. R., Henry, B., & Fox, J. (1990). Reduction of interference fringes in small multipass absorption cells by pressure modulation. *Applied Optics*, 29(7), 900–902. <https://doi.org/10.1364/AO.29.000900>
- [13] Silver, J. A., & Stanton, A. C. (1988). Optical interference fringe reduction in laser absorption experiments. *Applied Optics*, 27(10), 1914–1916. <https://doi.org/10.1364/AO.27.001914>
- [14] Kronfeldt, H. D. (1993, April). Piezo-enhanced multireflection cells applied for in-situ measurements of trace-gas concentrations. In *Lens and Optical Systems Design* (Vol. 1780, pp. 512–519). SPIE. <https://doi.org/10.1117/12.142854>
- [15] Liger, V. V. (1999). Optical fringes reduction in ultrasensitive diode laser absorption spectroscopy. *Spectrochimica Acta Part A: Molecular and Biomolecular Spectroscopy*, 55(10), 2021–2026. [https://doi.org/10.1016/S1386-1425\(99\)00074-8](https://doi.org/10.1016/S1386-1425(99)00074-8)
- [16] Webster, C. R. (1985). Brewster-plate spoiler: a novel method for reducing the amplitude of interference fringes that limit tunable-laser absorption sensitivities. *JOSA B*, 2(9), 1464–1470. <https://doi.org/10.1364/JOSAB.2.001464>
- [17] Li, C., Guo, X., Ji, W., Wei, J., Qiu, X., & Ma, W. (2018). Etalon fringe removal of tunable diode laser multi-pass spectroscopy by wavelet transforms. *Optical and Quantum Electronics*, 50, 1–11. <https://doi.org/10.1007/s11082-018-1539-4>
- [18] Li, C., Shao, L., Meng, H., Wei, J., Qiu, X., He, Q., Ma, W., Deng, L., & Chen, Y. (2018). High-speed multi-pass tunable diode laser absorption spectrometer based on frequency-modulation spectroscopy. *Optics Express*, 26(22), 29330–29339. <https://doi.org/10.1364/OE.26.029330>
- [19] Lee, L., Park, H., Ko, K. H., Kim, T. S., & Jeong, D. Y. (2010). Reduction of fringe noise in a multi-pass absorption cell by using the wavelength modulation technique. *Journal of the Korean Physical Society*, 57(2), 364–368. <https://doi.org/10.3938/jkps.57.364>
- [20] Nikodem, M., & Wsocki, G. (2012). Chirped laser dispersion spectroscopy for remote open-path trace-gas sensing. *Sensors*, 12(12), 16466–16481. <https://doi.org/10.3390/s121216466>

- [21] Winkowski, M., & Stacewicz, T. (2021). Optical interference suppression using wavelength modulation. *Optics Communications*, 480, 126464. <https://doi.org/10.1016/j.optcom.2020.126464>
- [22] Owen, M. (2007). *Practical signal processing*. Cambridge University Press.
- [23] Smith, S. W. (1997). *The Scientist and Engineer's Guide to Digital Signal Processing*.
- [24] Alduchov, O. A., & Eskridge, R. E. (1996). Improved Magnus form approximation of saturation vapor pressure. *Journal of Applied Meteorology and Climatology*, 35(4), 601–609. [https://doi.org/10.1175/1520-0450\(1996\)035<0601:IMFAOS>2.0.CO;2](https://doi.org/10.1175/1520-0450(1996)035<0601:IMFAOS>2.0.CO;2)

**Tadeusz Stacewicz** is a professor at the Faculty of Physics, University of Warsaw. His scientific activity are optics, laser spectroscopy methods for trace matter detection, laser generated plasma, and LIDAR techniques. He is currently conducting a project about trace matter detection by means of ultrasensitive laser absorption techniques: Cavity Ring-Down Spectroscopy (CRDS) and multipass spectroscopy. The project is focused on disease biomarkers detection in breath with spectroscopic techniques. His list of publications contains about 140 scientific papers, 183 conference communications and 33 invited conference talks as well as 5 books and 3 patents. According to the Web of Science Core Collection the citation number of his paper is about 880, H index = 16, average citation per item = 8.7.

**Mateusz Winkowski** is a Ph.D. student at the Faculty of Physics, University of Warsaw. His scientific activity concerns laser spectroscopy methods for trace matter detection, including electronics design, programming and signal analysis. He is presently focused on disease biomarkers detection in breath with spectroscopic techniques as a member of Tadeusz Stacewicz's team. Mateusz Winkowski graduated from both Warsaw University of Technology (Faculty of Electronics and Information Technology) and University of Warsaw (Faculty of Physics).